

Preliminary Title: Plasma Wakefield Acceleration

Veronica K. Berglyd Olsen

Department of Physics

University of Oslo

Norway



Dissertation Presented for the Degree of
Philosophiae Doctor (PhD) in Physics

July 2017

Abstract

Abstract

Acknowledgements

Acknowledgements

Contents

1	Introduction	1
1.1	Plasma Wakefield Acceleration	1
1.1.1	The Linear Regime	2
1.1.2	The Non-Linear Regime	2
1.2	Proton Driven Plasma Wakefield Acceleration	2
1.3	The Self-modulation Instability	2
1.4	Numerical Simulations of PWFA	2
2	A Wakefield Accelerator Experiment	3
2.1	Evolution of the Concept	3
2.2	The Advanced Wakefield Experiment (AWAKE)	3
2.2.1	AWAKE Run 1	3
2.2.2	AWAKE Run 2	3
2.3	The Self-modulation Instability in AWAKE	3
3	Simulations	5
3.1	Evolution of the Proton Beam	5
3.1.1	Studies with Pre-modulated Beam	5
3.1.2	Studies with Single Drive Bunch	5
3.2	Beam Loading and Energy Spread	5
3.2.1	The Linear Regime	5
3.2.2	The Quasi-linear Regime	5
3.3	Emittance Evolution	5
3.3.1	Beam Matching	5
3.3.2	The Quasi-linear + Linear Case	5
3.4	Optimising the Witness Beam	6
4	AWAKE Data Acquisition	7
4.1	Data Acquisition Classes for FESA	7
5	Summary and Conclusion	9

Publications

I	Loading of a Plasma-Wakefield Accelerator Section Driven by a Self-Modulated Proton Bunch, <i>Proceedings of IPAC 2015</i>	13
---	--	----

Contents

II	Loading of Wakefields in a Plasma Accelerator Section Driven by a Self-Modulated Proton Beam, <i>Proceedings of NAPAC 2016</i>	19
III	Data Acquisition and Controls Integration of the AWAKE Experiment at CERN, <i>Proceedings of IPAC 2017</i>	25
IV	Emittance Preservation of an Electron Bunch in a Loaded Quasi-Linear Plasma Wakefield, <i>Physical Review Accelerators and Beams</i>	31

Appendices

A	Particle in Cell (PIC)	43
A.1	Numerical Cherenkov	43
B	Data Analysis	45
B.1	Osiris Analysis Framework	45
B.1.1	OsirisAnalysis Core Objects	46
B.1.2	OsirisAnalysis Data Types	46
B.1.3	OsirisAnalysis Graphical Interface and Plots	46
	Bibliography	47

1 Introduction

Accelerating a particle beam in a plasma is an attractive concept because the plasma itself is capable of sustaining significantly higher accelerating fields than conventional RF structures. Conventional RF structures suffers electrical breakdowns at very high electric fields, and these breakdowns can over time damage the accelerator structures⁶. This puts an upper limit on the accelerating gradient of around 350 to 400 MV/m. The practical upper limit is however determined by the statistical probability of a breakdown and the acceptable number of breakdowns in a given period of time.⁹

1.1 Plasma Wakefield Acceleration

The principles behind plasma wakefield acceleration (PWFA) were formulated in the 1980s by Pisin Chen *et al.*⁷ Conceptually, the technique involves a beam of particles called the drive beam, travelling through a plasma of a given density. The beam generates strong longitudinal and transverse electric fields in its wake, of witch a trailing beam of particles draws energy in order to accelerate – thus we see a transfer of energy from one beam to another through plasma as the intermediate medium.

The trailing fields have a periodic structure determined by the plasma frequency, ω_{pe} , and wavelength, λ_{pe} ; given as

$$\lambda_{pe} = \frac{2\pi c}{\omega_{pe}}, \quad \omega_{pe} = \sqrt{\frac{n_0 e^2}{m_e \epsilon_0}}, \quad (1.1)$$

where n_0 is the initial plasma electron density, e is the elementary charge, m_e is the electron mass, and ϵ_0 is the vacuum permittivity.

It has been shown experimentally that energy can be transferred from one or two electron drive beams to a single electron witness beam.^{5,8,10} A limitation using an electron beams with a similar initial charge and energy for both drive and witness beam is that the witness beam will rapidly gain energy while the drive beam loses energy. This causes the witness beam to catch up with the drive beam, and the acceleration stops.

1.1.1 The Linear Regime

A point like charge travelling at a speed close to the speed of light, will generate fields in its wake^{7,11}:

$$E_z = -\frac{Q_b k_{pe}^2}{2\pi\epsilon_0} K_0(k_{pe}r) \cos(k_{pe}z - \omega_{pe}t) \quad (1.2)$$

$$E_r = \frac{Q_b k_{pe}^2}{2\pi\epsilon_0} K_1(k_{pe}r) \sin(k_{pe}z - \omega_{pe}t), \quad (1.3)$$

where Q_b is the charge of the beam, k_{pe} is the plasma wave number, and K_0 and K_1 are modified Bessel functions.

1.1.2 The Non-Linear Regime

Text

1.2 Proton Driven Plasma Wakefield Acceleration

Further details on proton driven plasma wakefield goes here.

1.3 The Self-modulation Instability

Stuff about SMI goes here

1.4 Numerical Simulations of PWFA

Stuff about Osiris and and all that jazz.

Reference to PIC appendix.

2 A Wakefield Accelerator Experiment

Text

2.1 Evolution of the Concept

Text

2.2 The Advanced Wakefield Experiment (AWAKE)

Text

2.2.1 AWAKE Run 1

Text

2.2.2 AWAKE Run 2

Text

2.3 The Self-modulation Instability in AWAKE

Text

3 Simulations

3.1 Evolution of the Proton Beam

Text

3.1.1 Studies with Pre-modulated Beam

Text

3.1.2 Studies with Single Drive Bunch

Text

3.2 Beam Loading and Energy Spread

Text

3.2.1 The Linear Regime

The ideal case from Tzoufras 2008.

3.2.2 The Quasi-linear Regime

Text

3.3 Emittance Evolution

Emittance is preserved in the linear regime

3.3.1 Beam Matching

Text

3.3.2 The Quasi-linear + Linear Case

Text

3.4 Optimising the Witness Beam

Bringing it all together.

4 AWAKE Data Acquisition

4.1 Data Acquisition Classes for FESA

Some text.

5 Summary and Conclusion

Text

Publications

Publication I

Loading of a Plasma-Wakefield Accelerator Section Driven by a Self-Modulated Proton Bunch

Abstract: We investigate beam loading of a plasma wake driven by a self-modulated proton beam using particle-in-cell simulations for phase III of the AWAKE project. We address the case of injection after the proton beam has already experienced self-modulation in a previous plasma. Optimal parameters for the injected electron bunch in terms of initial beam energy and beam charge density are investigated and evaluated in terms of witness bunch energy and energy spread. An approximate modulated proton beam is emulated in order to reduce computation time in these simulations.

Authors: Veronica K. Berglyd Olsen, Erik Adli (University of Oslo, Oslo, Norway), Patric Muggli (Max Planck Institute for Physics, Munich, Germany), Ligia D. Amorim, Jorge M. Vieira (Instituto Superior Technico, Lisbon, Portugal)

Publication: Proceedings of IPAC 2015, Richmond, Virginia, USA²

Date: 3rd to 8th of May, 2015

LOADING OF A PLASMA-WAKEFIELD ACCELERATOR SECTION DRIVEN BY A SELF-MODULATED PROTON BUNCH

V. K. Berglyd Olsen*, E. Adli (University of Oslo, Norway)

P. Muggli (Max Planck Institute for Physics, Munich, Germany)

L. D. Amorim, J. M. Vieira (Instituto Superior Technico, Lisbon, Portugal)

Abstract

We investigate beam loading of a plasma wake driven by a self-modulated proton beam using particle-in-cell simulations for phase III of the AWAKE project. We address the case of injection after the proton beam has already experienced self-modulation in a previous plasma. Optimal parameters for the injected electron bunch in terms of initial beam energy and beam charge density are investigated and evaluated in terms of witness bunch energy and energy spread. An approximate modulated proton beam is emulated in order to reduce computation time in these simulations.

INTRODUCTION

The AWAKE experiment [1] is a proof-of-principle demonstration of acceleration of an electron bunch to the TeV energy range in a single plasma section, using a proton bunch driver [2].

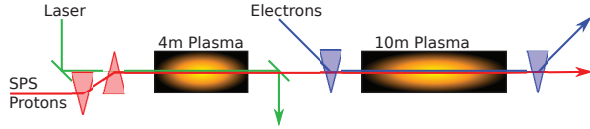


Figure 1: Simplified set-up of AWAKE Phase III. A long proton bunch experiences the SMI in a short plasma cell. The electron bunch is injected before the second plasma cell.

The AWAKE experiment proposes using a proton driver at 400 GeV, delivered by the SPS. The experiment is currently under construction at CERN, scheduled to start in late 2016. The SPS proton bunch is too long to generate a sufficiently strong wakefield [3]. A usable drive bunch needs to be close to the plasma wavelength λ_p in length; however, producing a short enough proton bunch is technically difficult.

The plasma wavelength and frequency are given by

$$\lambda_p = \frac{2\pi c}{\omega_p}, \quad \omega_p = \sqrt{\frac{N_p e^2}{m_e \epsilon_0}}, \quad (1)$$

where N_p is the plasma electron density, e is the elementary charge, m_e is the electron mass and ϵ_0 is the vacuum permittivity.

A proton bunch with $\sigma_{z,0} k_p \gg 1$, where $\sigma_{z,0}$ is the initial length of the bunch, will under certain conditions develop a self-modulation instability (SMI) when it travels through a plasma [4]. The proton bunch will then develop into a train of micro bunches with a period on the order of λ_p .

* v.k.b.olsen@fys.uio.no

In phase I of the AWAKE experiment the SMI of the proton bunch will be studied. In phase II, the proton wake will be studied using a long, externally injected electron bunch that will sample all phases of the wake. In phase III, acceleration of a short bunch in the wake of an already self-modulated proton beam will be studied, as illustrated in Fig. 1. In this paper we study the beam quality of a short electron bunch accelerated by an SMI proton wake in preparation for phase III of AWAKE.

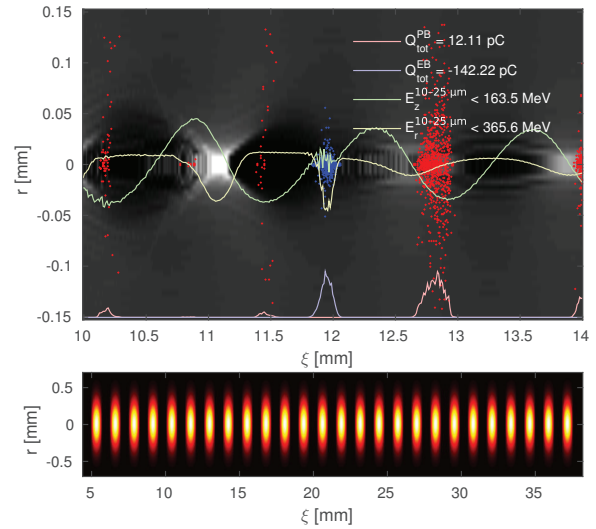


Figure 2: **Top:** An example showing the structure of the plasma electrons (grey) with a projection of the proton beam (red) and the electron bunch (blue) density on the bottom. The E_z (green) and E_r (yellow) fields have been overlaid on the plot. Shown is also a sample of electron (blue) and proton (red) macro particles. **Bottom:** An example of a pre-modulated proton drive beam at $t = 0$ plotted in terms of charge density.

SIMULATION SET-UP

All simulations in this paper have been performed using OSIRIS, a three-dimensional, relativistic, particle-in-cell code for modelling plasma based accelerators [5].

The parameter scans presented have all been run on a small scale test case with a shorter proton drive beam than AWAKE specifications. We simulate here only the second plasma stage in Fig. 1, assuming a pre-modulated proton beam profile with charge density function

$$\rho_{p^+}(\xi) = A \left[\frac{1}{2\sqrt{2}} + \cos(k_p \xi - \mu_1) \right] e^{-r^2/2\sigma_r}, \quad (2)$$

where A is a charge scaling factor, μ_1 is the centre position of the first micro bunch, $k_p = 2\pi\lambda_p^{-1}$ is the wave number, and $\xi = z - ct$ is the coordinates in a frame moving at the speed of light.

The length of the beam is limited by a step function to 33 mm. Negative density values for the density profile is ignored by OSIRIS. This gives a beam of 26 micro bunches of protons, as seen in the bottom plot of Fig. 2. The beam has a total initial charge of 2.6 nC, with an initial peak current per micro bunch of 135 A. For the proton beam $\sigma_r = 200 \mu\text{m} = 1.00 c/\omega_p$ in all simulations, where c/ω_p is the plasma skin depth.

The electron witness bunch is injected between micro bunches 20 and 21 of the drive beam, at $\xi \approx 12 \text{ mm}$, see Fig. 2. The charge density of the electron bunch is given by

$$\rho_e(\xi) = Ae^{-(\xi-\mu)^2/2\sigma_z}e^{-r^2/2\sigma_r}. \quad (3)$$

For the electron bunch $\sigma_r = 105 \mu\text{m} = 0.52 c/\omega_p$, and $\sigma_z = 40 \mu\text{m} = 0.2 c/\omega_p$ in the cases with a short electron bunch. The plasma density at the beginning of the plasma section for all these simulations is $N_p = 7 \times 10^{14} \text{ cm}^{-3}$.

BEAM INJECTION

While the peak-to-peak distance between micro bunches of the self-modulated proton beam corresponds closely to the plasma wavelength λ_p , it is not constant along the length of the beam [6]. A brief study of the SMI of both full scale and small scale proton beams, using Fourier transform and Wavelet analysis, revealed that the fundamental frequency was slightly lower than one k_p .

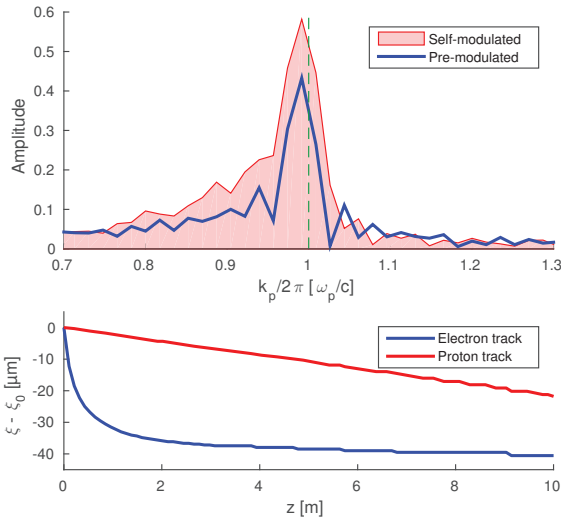


Figure 3: **Top:** The Fourier transform of the proton beam after 10 m of plasma for a self- and pre-modulated beam. The green line indicates $k_p = 2\pi/\lambda_p$. **Bottom:** Typical drift of a proton and electron macro particle through the plasma in respect to c .

To minimise further SMI development with a pre-modulated beam, the micro bunch distance was reduced

to $0.9939 k_p$, which produced a very good fit to the actual SMI for our test case, see Fig. 3.

An electron bunch of low MeV range initial energy will, due to its low gamma factor compared to the 400 GeV proton beam, slip backwards. In order to minimise this effect we set the initial energy of the electron bunch to 30 MeV, a little higher than AWAKE parameters. Typical slip for the beams through 10 m of plasma is illustrated in Fig. 3.

Staying in phase with the drive beam is essential to optimise energy transfer. Establishing an optimal injection point of the electron bunch was achieved by using bunches with length in the order of one λ_p , and tracking a selection of the electrons with optimal energy gain back to $z = 0$.

BEAM LOADING AND ENERGY SPREAD

In a plasma wakefield accelerator, the witness bunch should be accelerated at high efficiency while preserving a low energy spread. Beam loading in the linear regime can be calculated by the linear addition of fields. Only very narrow electron bunches, with $\sigma_r \ll c/\omega_p$, can maintain low energy spread and emittance [7, 8].

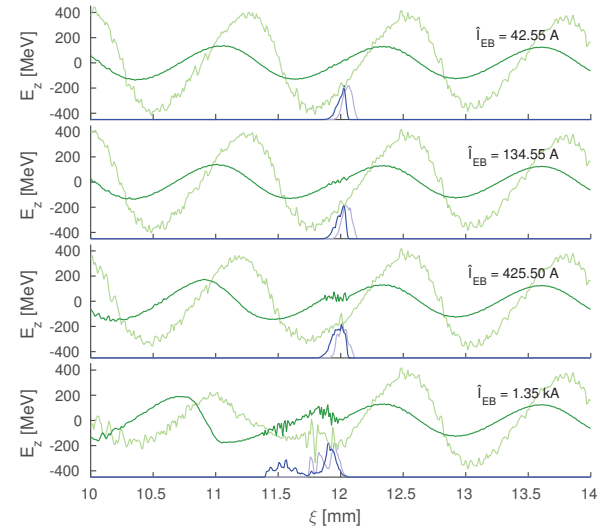


Figure 4: Comparison between the E_z field at 1 m (light green) and 10 m (dark green) of plasma for four different electron bunch currents. The fields are averages over a region $10 - 25 \mu\text{m}$ from the axis. A dimensionless plot of the charge density of the electron bunch is added in blue.

In the non-linear blowout regime, the plasma electrons are blown out by the drive beam, leaving behind a uniform region of plasma ions. The ions pull the electrons back towards the axis, forming a bubble with length on the order of the plasma wavelength [8, 9]. In this regime, the charge and current profile required to optimally load the wake can be estimated analytically. Optimal loading results in a flat E_z field across the bunch with high wake to beam energy transfer efficiency. There is a trade-off between the number of particles that can be accelerated and the accelerating gradient, as discussed in detail by Tzoufras et. al [10].

3: Alternative Particle Sources and Acceleration Techniques

A22 - Plasma Wakefield Acceleration

The beam-plasma interaction studied in this paper has similarities with the above blowout regime, but the train of micro bunches produces a more complex wakefield [4]. We have studied the beam loading through simulations. Based on beam loading in the blowout regime, we use as starting point for the studies a witness bunch with the same peak current as the initial peak current of one proton micro bunch, 135 A. We then performed a scan with logarithmic steps of current from 13.46 A to 13.46 kA. A selection of these are shown in Fig. 4, significant loading of the E_z field does occur when the witness bunch has significantly higher current than the proton beam. An approximate flattening of the field is observed when the witness bunch current is about 3 times higher than the initial micro bunch current, as shown in Fig. 4c. For higher witness bunch currents, we observe that the field from the witness bunch itself starts to dominate the wake it experiences, as expected. The trailing part of the electron bunch is therefore decelerated, as shown for example in Fig. 4d.

We notice that constant loading as the drive and witness bunch propagate in the plasma is not possible, as protons keep being ejected radially throughout the plasma, eating up the micro bunches from the front. This leads to the energy gain levelling off after approximately 4 m of plasma, turning into energy loss as the dephasing between the electron bunch and the E_z fields becomes too large. The phase difference of E_z at 1 m and 10 m is shown in Fig. 4. The mean energy gain (816.2 MeV) and relative energy spread (12%) of the electron bunch, as it travels through the plasma, is visible in blue in Fig. 5, showing a case with peak electron current of 425.5 A. The peak current of a micro bunch after 10 m of plasma, within one skin depth of the axis, is only 45 A.

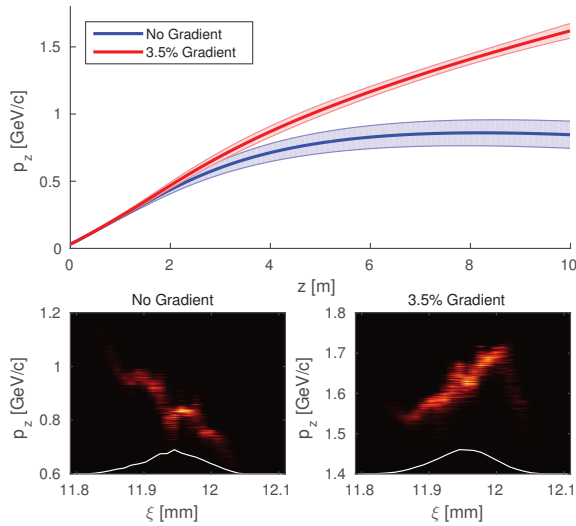


Figure 5: **Top:** Energy gain through 10 m of plasma for a short electron witness bunch with $\sigma_z = 40 \mu\text{m}$ and $I = 425.5 \text{ A}$, for the case of no plasma gradient and 3.5% plasma gradient. **Bottom:** $\xi - p_z$ phase plot for both simulations at the end of the plasma.

PLASMA GRADIENT

Due to the backwards drift of the E_z field, the electron bunch falls out of optimal phase after a few metres of plasma. It is possible to stabilise the accelerating bucket by gradually increasing the plasma density. We performed a scan of plasma gradients ranging from 0% to 10% along 10 m of plasma, with a square bunch of length λ_p . We found that a gradient of $0.2 - 0.3 \times 10^{14} \text{ cm}^{-3}$ (3 – 4%) per metre plasma for our initial density of $7 \times 10^{14} \text{ cm}^{-3}$, produced the highest energy gain for the electrons with optimal phase. By tracking some of these electrons back to their injection point, we could move the centre of the short bunch and do a new simulation comparing no gradient to a 3.5% gradient. The best result was for a gradient with a density at 10 m of $7.245 \times 10^{14} \text{ cm}^{-3}$ (3.5%), see Fig. 5 and Table 1.

Table 1: Electron Bunch Energy After 10 m of Plasma

Energy	No Gradient	3.5% Gradient
Mean	846.20 MeV	1618.77 MeV
RMS	101.23 MeV	54.93 MeV
RMS/Mean	11.96 %	3.39 %

CONCLUSION

We have studied beam loading of a SMI proton wake. A scan of electron witness bunch charges over three orders of magnitude revealed that a witness bunch peak current of about a factor 3 higher than the initial peak current of one proton micro bunch was optimal for flattening the wakefield. It is important to note that protons keep getting ejected radially, resulting in a loss of proton charge close to the axis, as the beam travels through the plasma. This decreases the current of a micro bunch by a factor of ~ 3 in the no gradient case.

The electron bunch does not stay in optimal phase for very long as the E_z field starts to drift significantly after 2 – 4 m of plasma. In most simulations the bunch ends up around the zero point of the E_z field, and the energy gradient flattens, and in some cases turns negative. For our optimal case of phase and charge, this effect could to a large degree be counteracted by a 3.5% gradient of the plasma, which forces a positive phase shift of the E_z field, keeping the electron bunch synchronous with the accelerating phase of the wake.

ACKNOWLEDGEMENT

The authors would like to acknowledge the OSIRIS Consortium, consisting of UCLA and IST (Lisbon, Portugal) for the use of OSIRIS, for providing access to the OSIRIS framework.

REFERENCES

- [1] AWAKE Collaboration et al., Plasma Phys. Control. Fusion **56**, 084013 (2014).

- [2] E. Gschwendtner et al., in Proceedings of IPAC2014 (2014), pp. 582–585.
- [3] N. Kumar et al., Phys. Rev. Lett. **104**, 255003 (2010).
- [4] A. Caldwell et al., Phys. Plasmas **18**, 103101 (2011).
- [5] R. A. Fonseca et al., in *Computational science — ICCS 2002*, edited by P. M. A. Sloot et al., Lecture Notes in Computer Science 2331 (Springer Berlin Heidelberg, 2002), pp. 342–351.
- [6] J. Vieira et al., Phys. Plasmas **19**, 063105 (2012).
- [7] T. Katsouleas et al., Part. Acc. **22**, 81–99 (1987).
- [8] M. Tzoufras et al., Phys. Rev. Lett. **101**, 145002 (2008).
- [9] W. Lu et al., Phys. Plasmas **13**, 056709 (2006).
- [10] M. Tzoufras et al., Phys. Plasmas **16**, 056705 (2009).

Publication II

Loading of Wakefields in a Plasma Accelerator Section Driven by a Self-Modulated Proton Beam

Abstract: Using parameters from the AWAKE project and particle-in-cell simulations we investigate beam loading of a plasma wake driven by a self-modulated proton beam. Addressing the case of injection of an electron witness bunch after the drive beam has already experienced self-modulation in a previous plasma, we optimise witness bunch parameters of size, charge and injection phase to maximise energy gain and minimise relative energy spread and emittance of the accelerated bunch.

Authors: Veronica K. Berglyd Olsen, Erik Adli (University of Oslo, Oslo, Norway), Patric Muggli (Max Planck Institute for Physics, Munich, Germany and CERN, Geneva, Switzerland), Jorge M. Vieira (Instituto Superior Technico, Lisbon, Portugal)

Publication: Proceedings of NAPAC 2016, Chicago, Illinois, USA³

Date: 9th to 14th of October, 2016

LOADING OF WAKEFIELDS IN A PLASMA ACCELERATOR SECTION DRIVEN BY A SELF-MODULATED PROTON BEAM

V. K. Berglyd Olsen*, E. Adli (University of Oslo, Oslo, Norway)

P. Muggli (Max Planck Institute for Physics, Munich, Germany and CERN, Geneva, Switzerland)

J. M. Vieira (Instituto Superior Technico, Lisbon, Portugal)

Abstract

Using parameters from the AWAKE project and particle-in-cell simulations we investigate beam loading of a plasma wake driven by a self-modulated proton beam. Addressing the case of injection of an electron witness bunch after the drive beam has already experienced self-modulation in a previous plasma, we optimise witness bunch parameters of size, charge and injection phase to maximise energy gain and minimise relative energy spread and emittance of the accelerated bunch.

INTRODUCTION

The AWAKE experiment at CERN proposes to use a proton beam to drive a plasma wakefield accelerator with a gradient on the order of 1 GeV/m to accelerate an electron witness beam [1, 2].

In this paper we present two simulation configurations with a modified proton drive beam based on the baseline parameters for the AWAKE experiment. The drive beam is delivered from the SPS accelerator at CERN at an energy of 400 GeV/c, a bunch length $\sigma_z = 12$ cm, and $\sigma_{x,y} = 200 \mu\text{m}$. [3].

The baseline plasma electron density n_{pe} for AWAKE is $7 \times 10^{14} \text{ cm}^{-3}$. The corresponding plasma wavelength $\lambda_{pe} = 2\pi c/\omega_{pe} = 1.26$ mm, where $c/\omega_{pe} = 200 \mu\text{m}$ is the plasma skin depth, and ω_{pe} is the plasma frequency given as $[n_{pe}e^2/m_e\epsilon_0]^{1/2}$.

In order to generate a suitable wakefield, the drive beam must be shorter than λ_{pe} . This is not achievable for the SPS proton beam. In order to use such a beam to drive a wakefield we exploit the self-modulation instability (SMI) that can occurs when the beam travels through a plasma and $\sigma_z \gg \lambda_{pe}$. The SMI modulates the beam at a period of $\approx \lambda_{pe}$ [4], allowing us to inject the witness beam in an optimal bucket between two such proton micro bunches.

BEAM LOADING

A particle beam at high energy travelling through a plasma will excite a plasma wave in its wake, and the plasma can sustain a very high accelerating gradient [5]. It is possible to accelerate a secondary beam by extracting energy from this wakefield, thus transferring energy from a drive beam to a trailing witness beam. Such an accelerator design was first proposed by Chen in 1985 [6]. However, there are some challenges in this transfer of energy from drive to witness beam.

* v.k.b.olsen@fys.uio.no

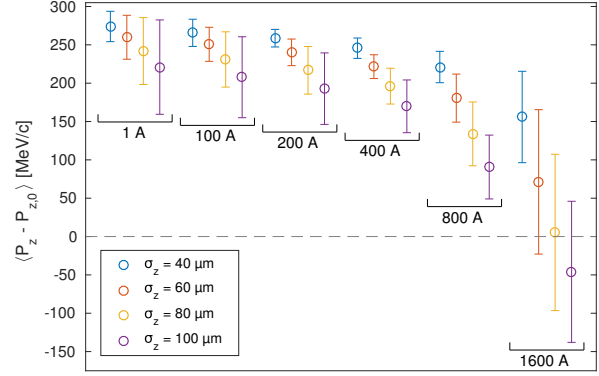


Figure 1: Energy gain and spread for a series of witness beams after ≈ 1.1 m of plasma. The initial momentum of the witness beam is 217.8 MeV/c. Mean momentum and RMS spread is calculated for all macro particles in the PIC simulation.

One such challenge stems from the witness beam generating its own field, modifying the E_z -field behind it such that the particles in the tail will be accelerated less than those in the front. This causes an increase in energy spread in the beam [7]. This effect can in theory be corrected for by shaping the witness beam. An optimally shaped and positioned beam, such as a triangular beam, can flatten the wakefield such that change in energy spread is effectively zero [8]. However, this requires beam shapes that are difficult to produce experimentally.

BEAM LOADING OF SMI WAKEFIELDS

For AWAKE, most of the SMI evolves during the first stage of $z < 4$ m [2]. This evolution results in a phase change of the wakefields that causes the optimal point for acceleration to drift backwards relative to the witness beam [9, 10].

In our current study we have restricted ourselves to Gaussian witness beams, and seek to demonstrate through simulations how small energy spread can still be achieved by optimally loading the field. The first set of simulations presented uses a subset of 26 micro bunches resulting from the self-modulation that occurs in the previous plasma stage. The pre-modulated beam does undergo further evolution as the envelope function does not fully match the SMI beam, but we only look at the first ≤ 3 m of this stage, before the phase change starts to dominate [11]. All simulations have been done using OSIRIS 3.0 [12].

A second set of proposed simulations for the second plasma stage will use a single drive beam scaled to produce an accelerating field of 500 MV/m, but with its transverse evolution inhibited in order to study the loading of the field produced by the witness beam alone. The drive beam is short, $\sigma_z = 40 \mu\text{m} \ll \lambda_{pe}$, which is well below the SMI limit.

MULTI DRIVE BUNCH SIMULATIONS

In the multiple drive bunch simulations we assume self-modulation has occurred in a previous stage, and approximate the resulting proton beam in the second stage where acceleration of the witness beam occurs. In this first series of studies we have used a short series of 26 proton bunches with a clipped cosine envelope. This setup is about 10 times shorter than full scale AWAKE simulations, allowing us to run more detailed parameter scans. The setup is described in more detail in our IPAC'15 proceedings, where we looked at beam loading as well as the evolution of the proton beam in a 10 m plasma section [11].

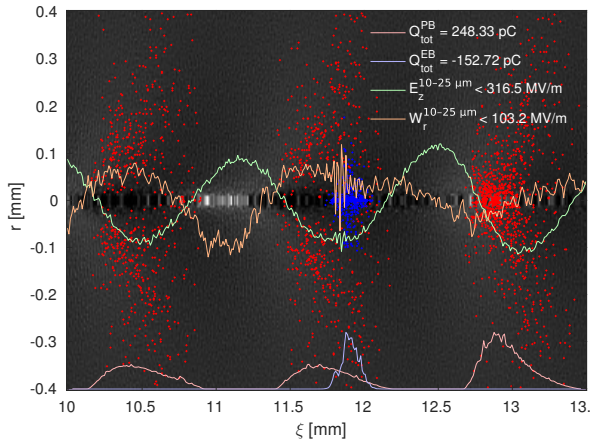


Figure 2: Loading of the field after ≈ 1.1 m of plasma for a 400 A/60 μm electron beam. A sample of electrons (blue) and protons (red) are plotted with their respective projection at the bottom. The total charge within the region of the plot is given as the first two lines of the legend. The longitudinal e-field E_z is shown in green. The transverse wakefield $W_r = E_r - v_z B_\theta$ is shown in orange, where $v_z = c$ is the moving frame of the simulation. The fields are averages over 15 μm near the axis.

The quality and energy of the accelerated witness beam depends on both its position in relation to the field as well as how uniform the field is in the region where the beam is located. We have matched the initial γ of both witness and drive beam in order to avoid initial slipping of the witness beam with relation to the wakefield. The accelerating phase of the field is in the order of $\lambda_{pe}/4 \approx 300 \mu\text{m}$ in length, which puts a constraint on the longitudinal size of the witness beam. The transverse size $\sigma_r = 100 \mu\text{m}$, however we observe in simulations that the beam shrinks by a factor of 4 – 6 as it enters the plasma section. This again results in a sharp

increase in charge density. A scan of different beam sizes and initial beam current and their corresponding energy gain and spread is shown in Fig. 1.

The best result in terms of total energy spread is for the 40 μm beam of an initial current of 200 A, and for the 60 μm beam of an initial current of 400 A. The former beam carries 67 pC and the latter beam 200 pC. As we want to load the field as close to its maximum as possible, this comes at a cost as the tail of the beam will extend beyond the optimal point into the defocusing region of the wakefields. Fig. 2 shows a snapshot of the 60 μm /400 A simulation from Fig. 1. The longitudinal field is nearly flat as a result of the loading.

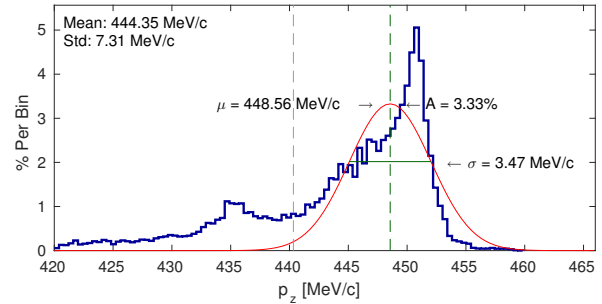


Figure 3: Electron beam momentum spread after ≈ 1.1 m of plasma for the 400 A/60 μm beam. 75 % of the beam charge is accelerated to more than 440 MeV/c, the vertical grey line. The fit is applied to the data above this line, $R^2 = 0.755$.

A closer look at the energy spread in Fig. 3 reveals that ≈ 75 % of the beam is accelerated in this region, with a long tail in energy. This case is not only optimal in terms of beam loading, but also in energy spread of the bulk of the beam of 150 pC. For that part of the beam in front of the grey line we get a relative energy spread $\sigma_{P_z}/[P_z - P_{z,0}] = 1.5$ %. The tail of the beam in terms of energy is lagging behind as it is experiencing defocusing and being pushed outwards and eventually lost from the plasma channel. This loss of beam in the tail can be counteracted by shaping the beam, and making the backwards half $\sigma_z = 20 \mu\text{m}$ and keeping the forward half at $\sigma_z = 60 \mu\text{m}$. In simulations this has reduced this loss to 4 – 5 %. However, such shaping of the beam is technically difficult.

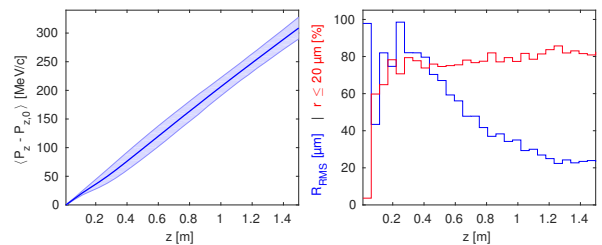


Figure 4: The 400 A/60 μm electron beam as it travels through plasma. The left plot shows the mean energy of the beam with the RMS energy spread as a shaded bar. The right plot shows the RMS radius in blue, and the percentage of macro particles the are within 20 μm of the axis in red.

The relative energy spread of 1.5 % is still undesired. The witness beam in these simulations is initiated with no energy spread in the longitudinal direction. Fig. 4 shows that for our best case the energy spread we see mainly develops in the first 20 cm of plasma. As the right plot illustrates, the transverse RMS size of the beam shrinks by a factor of 5 over the first metres of plasma, but already after a few centimetres about 80 % of the charge is found near the axis. It is this more compact beam that optimally loads the field, and for the first 20 cm the field is under-loaded, probably causing the increase in energy spread. This, however, needs to be studied further.

SINGLE DRIVE BUNCH SIMULATIONS

In order to study the loading of the accelerating e-field in more detail, a second set of simulations have been set up where we have a single proton drive bunch driving a wakefield on the order of 500 MV/m, which is the magnitude of the field we expect to see in the second plasma stage of AWAKE Run 2, based on simulations [13, 14].

This series of simulations is set up in such a way that the accelerating field is as static as possible in order to eliminate other factors than the beam loading by the witness bunch. To achieve this, the proton bunch is prevented from evolving transversely by setting the proton mass to a much higher value than its real value. The gamma of the drive and witness bunches are again matched to prevent dephasing.

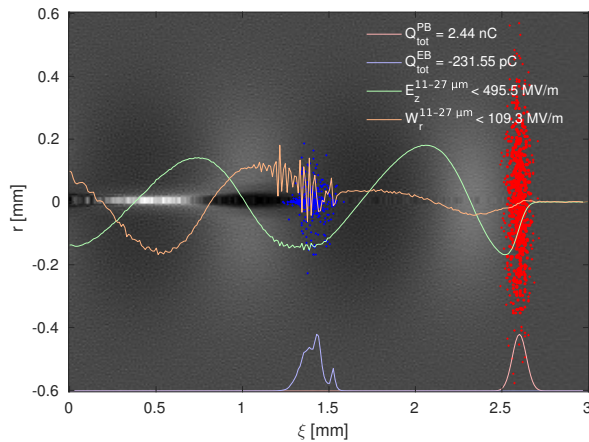


Figure 5: Loading of the field after ≈ 28 cm of plasma for a 500 A/60 μm electron beam. As in Fig. 2 a sample of electrons (blue) and protons (red) are plotted with their respective projections, and the E_z and W_r wakefields are shown.

This provides a much cleaner environment to study the effects of beam loading from the electron beam alone without any evolution caused by the proton beam. Fig. 5 shows an example of this setup. It reproduces the transverse wakefields we saw in our 26 bunch simulations. We also see a shrinking of the witness beam in the first few centimetres, which, together with emittance evolution, is the focus of this next stage of on-going simulation studies.

CONCLUSION AND CONTINUATION

There are a number of challenges with accelerating an electron beam by a self-modulated proton beam in plasma. Not only does the continued evolution of the proton beam affect the wakefield and thus the acceleration of the witness beam, but the evolution of the witness beam itself affects the wakefields, causing among other things, energy spread. However, by tuning the charge density of the beam, this loading of the field can be used to prevent continuing growth in energy spread provided the phase of the wakefield does not evolve too much.

This is an on-going study, and we are currently looking into the cause of the growth of energy spread. It is worth noting that we have so far run these simulations with an unmatched witness beam. We do see emittance growth in this same region where energy spread increases, but further studies are needed to properly understand the numerical contribution to both these effects.

ACKNOWLEDGEMENTS

The authors would like to acknowledge the OSIRIS Consortium, consisting of UCLA and IST (Lisbon, Portugal), for providing access to the OSIRIS framework.

The numerical simulations have been possible through access to the Abel supercomputer maintained by UNINETT Sigma2 AS, and financed by the Research Council of Norway, the University of Bergen, the University of Oslo, the University of Tromsø and the Norwegian University of Science and Technology. Project code: nn9303k.

REFERENCES

- [1] A. Collaboration, *et al.*, *Plasma Phys. Control. Fusion* 56, 084013 (2014).
- [2] A. Caldwell, *et al.*, *Nucl. Instr. Meth. Phys. Res. A* 829, 3–16 (2016).
- [3] E. Gschwendtner, *et al.*, *Nucl. Instr. Meth. Phys. Res. A* 829, 76–82 (2016).
- [4] N. Kumar, *et al.*, *Phys. Rev. Lett.* 104, 255003 (2010).
- [5] E. Esarey, *et al.*, *IEEE Transactions on Plasma Science* 24, 252–288 (1996).
- [6] P. Chen, *et al.*, *Phys. Rev. Lett.* 54, 693–696 (1985).
- [7] S. Van der Meer, tech. rep. CERN/PS/85-65 (AA), CLIC Note No. 3 (1985).
- [8] T. Katsouleas, *et al.*, *Part. Acc.* 22, 81–99 (1987).
- [9] A. Pukhov, *et al.*, *Phys. Rev. Lett.* 107, 145003 (2011).
- [10] C. B. Schroeder, *et al.*, *Phys. Rev. Lett.* 107, 145002 (2011).
- [11] V. K. B. Olsen, *et al.*, in *Proceedings of IPAC2015* (2015), pp. 2551–2554.
- [12] R. A. Fonseca, *et al.*, in *Computational Science — ICCS 2002*, 2331 (Springer Berlin Heidelberg, 2002), pp. 342–351.
- [13] A. Collaboration, *et al.*, tech. rep. CERN-SPSC-2016-033 (2016).
- [14] E. Adli, *et al.*, in *Proceedings of IPAC2016* (2016), pp. 2557–2560.

Publication III

Data Acquisition and Controls Integration of the AWAKE Experiment at CERN

Abstract: The AWAKE experiment has been successfully installed in the CNGS facility at CERN, and is currently in its first stage of operation. The experiment seeks to demonstrate self-modulation of an SPS proton beam in a rubidium plasma, driving a wakefield of several gigavolt per meter. We describe the data acquisition and control system of the AWAKE experiment, its integration into the CERN control system and new control developments specifically required for AWAKE.

Authors: Veronica K. Berglyd Olsen (University of Oslo, Oslo), Spencer J. Gessner, Jozef J. Batkiewicz, Stephane Deghaye, Edda Gschwendtner (CERN, Geneva, Switzerland), Patric Muggli (Max Planck Institute for Physics, Munich, Germany and CERN, Geneva, Switzerland)

Publication: Proceedings of IPAC 2017, Copenhagen, Denmark⁴

Date: 14th to 19th of May, 2017

DATA ACQUISITION AND CONTROLS INTEGRATION OF THE AWAKE EXPERIMENT AT CERN

Veronica K. Berglyd Olsen*, University of Oslo, Oslo, Norway
 Jozef J. Batkiewicz, Stephane Deghay, Spencer J. Gessner, Edda Gschwendtner,
 CERN, Geneva, Switzerland
 Patric Muggli, Max Planck Institute for Physics, Munich, Germany and
 CERN, Geneva, Switzerland

Abstract

The AWAKE experiment has been successfully installed in the CNGS facility at CERN, and is currently in its first stage of operation. The experiment seeks to demonstrate self-modulation of an SPS proton beam in a rubidium plasma, driving a wakefield of several gigavolt per meter. We describe the data acquisition and control system of the AWAKE experiment, its integration into the CERN control system, and new control developments specifically required for AWAKE.

device settings and acquired data, as well as subscription to any further data updates [3].

INTRODUCTION

AWAKE is an Advanced Wakefield Experiment designed to demonstrate proton driven plasma wakefield acceleration utilising a 400 GeV proton drive beam from the Super Proton Synchrotron at CERN [1]. The first phase of the experiment has been successfully installed in the former CNGS facility, and was commissioned in October and November 2016.

The first phase of AWAKE is intended to demonstrate the self-modulation instability in the proton drive beam [2], and we had a first short 48 hour run with rubidium plasma and protons in December 2016. Further three weeks of beam time are scheduled at the end of May and in August 2017. The installation of the electron beam phase is scheduled to be completed in September 2017, with first physics expected in November.

CERN CONTROL SYSTEM

Located at CERN, AWAKE is taking advantage of the extensive support infrastructure that already exists for experiments. This also includes integration into the CERN control system.

The Large Hadron Collider is controlled through the Front End Software Architecture (FESA), developed at CERN. This software framework has been extended and generalised in FESA3 to be usable by other experiments as well. FESA device classes are developed based on standardised and modular code tailored for each specific device. These classes are split into a real time and a server process. The real time process is intended to access the hardware directly, and in addition provides access to internal and external timing as well as information from other device classes. The server process provides an interface for get and set operations for

Figure 1: The CERN Control System is structured in three main layers. The Front End Layer consists of VME crates, PCs and PLCs dealing with high performance data acquisition and real time processing. These communicate with application, database and file servers as well as central timing on the Business Layer via the Controls Middleware. Graphical user interfaces and database access are found on the Presentation Layer, and interact with the Business Layer via Java APIs [4].

FESA classes run on Front End Computers (FEC), which run on the Linux operating system. The data from these classes are fed to both data logging systems and control room displays and interfaces as outlined in Fig. 1.

DATA ACQUISITION FOR WINDOWS BASED INSTRUMENTS

The AWAKE experiment has largely been integrated into this infrastructure through direct hardware access between the instruments and the FESA framework. However, some of the instruments depend on proprietary software that is not supported by the standard Front End Computer platform running on Scientific Linux. In order to get around this, and to avoid writing new software, data from three of the instruments currently have to be written to files on shared folders on Windows computers. These files are then imported by designated FESA file reader classes running on CERN supported FECs.

Three instruments currently require software or drivers only available for the Windows operating system:

* v.k.b.olsen@cern.ch

AWAKE uses Mach-Zehnder type interferometers to measure and calculate the vapour density at either end of the 10 m rubidium plasma cell. The acquired interferogram is stored as a file from the instruments software, and a fitting algorithm is applied to calculate the density to within at least $\pm 0.5\%$ relative accuracy [5]. As the fitting is too computationally heavy to run in real time, the fitting is not currently done by the file reader, but will be performed by a separate FESA class running on a dedicated computer.

The rubidium plasma is ionised by a 780 nm, 4.5 TW peak power laser with a pulse length of 100–120 fs [6]. The pulse length is measured by a single shot optical autocorrelator [7]. The autocorrelator itself is a commercial product, and we extract the data directly from its camera through its Windows drivers. On the local computer we compute the projection and fit it with a sech^2 function using Levenberg-Marquardt. We then write the projection, fit, pulse width and the full image to a binary file.

In addition, we have a 4-channel Tektronix oscilloscope with 23 GHz analogue bandwidth and a 50 GSa sampling rate per channel. The oscilloscope is used to measure real time signals from various Schottky diodes installed in a proton beam diagnostic setup downstream of the plasma cell. They measure Coherent Transition Radiation (CTR) emitted in the microwave band. We use proprietary Windows software to automatically save all channel data files at each event trigger.

Figure 2: The FESA file reader classes written specifically for AWAKE all operate in the same way. A process polls a dedicated watch folder every 500 ms for new files. The file content is verified according to the instruments' expected format, and either imported and archived, or moved to a dropped folder for later manual control. Imported data is immediately made available on the CMW interface to subscribed services [8].

These instruments require their own FESA class to handle their respective file formats. However, each of these classes operates in the same way, and therefore only requires individual data parsing code. A flow chart illustrating their operation is shown in Fig. 2. The beam cycle time for the experiment itself is around 30 seconds [6], but some of the instruments may be required to run at a higher frequency. The 500 ms delay is both chosen to allow for a ≤ 1 Hz data acquisition frequency with some margin allowed for file system response time, as well as to ensure there is no significant

delay between the time the file is written and when the data is available to the data logging layer. The class polls a dedicated watch folder and attempts to import all files present in reverse chronological order. This is to ensure all data is imported in case of for instance a network interruption. Valid files are then parsed, the data forwarded, and the file itself moved to an archive folder. The original file name of the imported file, as well as its creation time, is stored with the imported data. In the event of an invalid file, a warning is raised and the file is moved to a dropped files folder for later manual verification.

PXI DIGITAL CAMERA SYSTEM

AWAKE uses the analogue camera system provided by the CERN BI group to monitor the proton beam at BTV stations along the beam line. The analogue camera system is radiation hard and requires minimal mechanical upkeep. However, the system is asynchronous to beam extractions. It acquires frames at a fixed rate of 50 FPS and records the frame corresponding to beam extraction. This method of acquisition is not ideal for AWAKE, because AWAKE uses scintillating Chromox screens to image the beam. The scintillation has a long decay time of 140 ms, which is longer than the frame exposure time of 20 ms. This means that under identical experimental conditions, the recorded beam intensity on the screen will vary, simply because the analogue frame is not synced with the beam arrival time.

In addition to this issue, the analogue cameras cannot acquire data at 10 Hz, which is the repetition rate of the laser. For purposes of feedback and stability, it is critical to monitor the laser at this frequency. A digital camera system was implemented to monitor the laser. The camera server is a PXI crate made by National Instruments, and it comprises a trigger and timing system as well as GigE framegrabbers. The digital cameras are made by Basler Ace, and the system supports both CCD and CMOS sensors in a variety of sizes. The image data and camera power are both delivered by a GigE connection using the Power-over-Ethernet (PoE) standard.

The digital camera system was implemented at the laser merging point of the beamline and survived the radiation received during operations in 2016. Because of this success, the digital cameras are being implemented along the beamline to measure both the particle and laser beams. The cameras will be monitored for radiation exposure at areas where high doses are expected in order to understand the total integrated dose (TID) and the single event upset rate (SEU).

EVENT BUILDER

Devices at AWAKE can be read synchronously with SPS beam extractions or asynchronously between extractions. The synchronous/asynchronous distinction depends on the device. For instance, BPMs are read out only when the proton beam is present, but the temperature probes for the Rubidium cell are read out continuously in one second inter-

vals. All of the data from the AWAKE and SPS diagnostics are recorded by the logging system and it is possible to reconstruct the experiment after the fact. It is also desirable to have fast event reconstruction. In order to facilitate this process, the Event Builder was developed to take a “snapshot” of the experiment at the time of the SPS extraction. The Event Builder is subscribed to the key experimental diagnostics, and records their values at the time of extraction, thus providing an instantly correlated dataset comprising both the synchronous and asynchronous variables.

The Event Builder is a JAVA client that is able to subscribe to any variable exposed by the CMW. The Event Builder includes a time-out feature that waits for devices to return data following an extraction. Once the time-out ends, the Event Builder collects the data from all devices and writes them to an HDF5 file, which can be analysed instantly. This data is also copied to the CERN EOS system once per day.

SUMMARY

The integration of the AWAKE experiment into the CERN control system posed a number of challenges. CERN Front End Computers run on Scientific Linux, a platform not supported by all of our instruments. The straight forward solution was to let the Windows based instruments write data dump files on their respective computers, and then use the standard CERN Front End Software Architecture framework to develop file reader classes that can import these via shared network folders.

Due to the relatively large time interval between events, roughly 30 s, the data can be gathered based on time stamps

and collected per event in HDF5 files by an Event Builder. These event files are available immediately after an event, as well as backed up and stored for later analysis.

AWAKE uses many of CERN’s standard analogue and radiation hard cameras. However, these cameras pose synchronisation issues as they have a fixed frame rate of 50 FPS. At critical points, AWAKE uses digital cameras with a trigger and timing system instead.

ACKNOWLEDGEMENTS

The authors would like to thank the AWAKE team at CERN, as well as the CERN Beams, Engineering and Technical Departments for all their assistance in getting the experiment up and running.

REFERENCES

- [1] E. Gschwendtner, et al., in Proceedings of IPAC 2014 (2014), pp. 582–585.
- [2] A. Caldwell, et al., Nucl. Instr. Meth. Phys. Res. A **829**, 3–16 (2016).
- [3] A. Schwinn, et al., in Proceedings of PCaPAC 2010 (2010), pp. 22–26.
- [4] R. Gorbosov, AWAKE Collaboration Meeting, Apr. 2013.
- [5] E. Öz, F. Batsch, and P. Muggli, Nucl. Instr. Meth. Phys. Res. A **829**, 321–325 (2016).
- [6] E. Gschwendtner, et al., Nucl. Instr. Meth. Phys. Res. A **829**, 76–82 (2016).
- [7] F. Salin, et al., Appl. Opt., AO **26**, 4528–4531 (1987).
- [8] V. K. Berglyd Olsen, 17th AWAKE Technical Board, Feb. 2016.

Publication IV

Emittance Preservation of an Electron Bunch in a Loaded Quasi-Linear Plasma Wakefield

Abstract: We investigate beam loading and emittance preservation for a high-charge electron beam being accelerated in quasi-linear plasma wakefield driven by a short proton beam. The structure of the wakefield is similar to that of a long, modulated proton beam. By selecting transverse and longitudinal electron beam parameters in order to appropriately load the wake, we show that the bulk of the electron beam can be accelerated without significant emittance growth.

Authors: Veronica K. Berglyd Olsen, Erik Adli (University of Oslo, Oslo, Norway), Patric Muggli (Max Planck Institute for Physics, Munich, Germany and CERN, Geneva, Switzerland)

Publication: Physical Review Accelerators and Beams

Date:

Emittance preservation of an electron beam in a loaded quasi-linear plasma wakefield

Veronica K. Berglyd Olsen* and Erik Adli
University of Oslo, Oslo, Norway

Patric Muggli
*Max Planck Institute for Physics, Munich, Germany and
CERN, Geneva, Switzerland*
(Dated: September 5, 2017)

We investigate beam loading and emittance preservation for a high-charge electron beam being accelerated in quasi-linear plasma wakefield driven by a short proton beam. The structure of the wakefield is similar to that of a long, modulated proton beam, such as the one being studied by AWAKE. We show that by exploiting two well known effects, full blow out of plasma electrons by the accelerated beam, and beam loading of the wake field, the electron beam can be accelerated without significant emittance growth.

I. INTRODUCTION

Beam driven plasma wakefield accelerators have the potential to offer compact linear accelerators with high energy gradients, and have been of interest for several decades [1]. A relativistic beam travelling through a plasma excites a strong longitudinal e-field that can be loaded by a trailing witness beam. With optimal beam loading, an increase in energy spread can be kept to a minimum. Acceleration of an electron witness beam by an electron drive beam has been demonstrated experimentally in the past [2–4]. AWAKE at CERN is a proof of concept proton driven plasma wakefield accelerator experiment [5].

A major challenge with plasma wakefield accelerators is, however, to produce an accelerated beam while keeping growth in energy spread and emittance as low as possible. In the well described linear case where the beam density n_b is much smaller than the plasma density n_0 , the non-linear transverse wakefields cause emittance growth of the accelerated beam. The beam will also see a transversely varying accelerating field causing increasing energy spread [6]. In the non-linear regime, where $n_b > n_0$, a bubble is formed by the transverse oscillations of the plasma electrons forming a sheet around an evacuated area leaving only ions. The ions, assumed stationary, form an ion channel creating a focusing force that varies linearly with radius. This produces an axially symmetric focusing force [7, 8].

A. Self-modulation as a Driver

A train of electron drive bunches with a separation λ_{pe} and a length $l_b \ll \lambda_{pe}$, where $\lambda_p = 2\pi c/\omega_{pe}$ and $\omega_{pe} = (n_0 e^2/m_e \epsilon_0)^{1/2}$, will produce a field E_z that increases for each drive bunch [1]. A tailing witness beam loading the peak accelerating phase of this field will gain energy from

the wakefield from all of the drive bunches. Acceleration of an electron witness beam driven by two electron drive beams has been demonstrated at Brookhaven National Laboratory [9].

The energy carried by electron drive bunches used in previous experiments were typically small – on the order of 100 J – and the propagation length typically < 1 m [3, 10]. The energy of a high-charge electron beam accelerated to 1 TeV, similar to the beam in the international linear collider with 1×10^{10} electrons, is 1.6 kJ. By using electron beams or lasers as drivers, a large number of plasma stages is required. How to efficiently stage plasma accelerators is challenging without reducing the effective gradient and spoiling the beam quality [11, 12]. Proton drive beams available at CERN carry significantly more energy, 19 kJ for the SPS beam [13], allowing for longer accelerator stages. However, the SPS beam is orders of magnitude longer than the plasma wavelengths needed for such applications. This issue is resolved by letting the proton beam undergo self-modulation before injecting the witness beam into one of the buckets in the modulated structure. This self-modulation instability is caused by the transverse fields generated by the beam acting upon the beam itself, causing regions of the beam to rapidly defocus [14]. The modulation frequency is close to that of the plasma, and leaves a train of proton bunches along the beam axis with a surrounding halo.

B. AWAKE Run 2

The AWAKE experiment, currently in its first stages of operation at CERN, uses the SPS beam at 400 GeV as its driver, and a nominal plasma density $7 \times 10^{14} \text{ cm}^{-3}$ [13]. This plasma density corresponds to a plasma wavelength $\lambda_{pe} = 1.26$ mm. The plasma density is matched to the SPS proton beam such that $k_{pe}\sigma_x = 1$, where $k_{pe} = 2\pi/\lambda_{pe}$ is the plasma wave number. The aim of the first phase of Run 1 of the experiment is to demonstrate self-modulation of the proton beam, and in 2018 to sample the wakefield with a long electron beam. The study presented here is for Run 2 [15], which aims to

* v.k.b.olsen@cern.ch

demonstrate acceleration of a short electron beam to high energy with a minimal increase in emittance and energy spread.

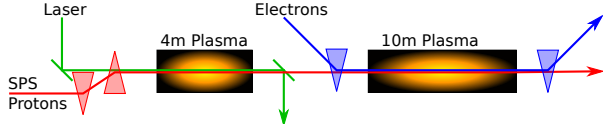


FIG. 1. A simplified illustration of the experimental setup for AWAKE Run 2. The SPS proton beam undergoes self-modulation in the first 4 m plasma cell. The electron witness beam is injected in one of the buckets, and undergoes acceleration in the second plasma cell [15, 16].

The preliminary design of Run 2 proposes to use two plasma sections, illustrated in figure 1. The first section of 4 m is the self-modulation stage where the proton beam undergoes self-modulation without the electron beam present. The electron witness beam will then be injected into the modulated proton beam before stage two, where it undergoes acceleration.

With this experimental design the self-modulated proton beam does not produce a full non-linear wakefield, and not all plasma electrons are therefore evacuated. The result is that the focusing force will not increase linearly with radius. The small size of the accelerating structure produced by the self-modulated beam also puts constraints on the size of the electron witness beam, and thus its charge and current – if we at the same time wish to prevent large energy spread. By matching the transverse size of the beam at a given emittance to the plasma density, we prevent large amplitude oscillations which may cause additional growth in energy spread as well as in emittance.

The key idea in this paper is that while the proton beam wake is not fully blown-out leading to non-linear focusing forces, the electron beam, if intense enough, may load the field and at the same time create its own ion bubble. As will be shown, exploiting these two well known effect, the electron beam can be accelerated, for long distances, without significant emittance growth.

II. METHOD

The main focus of this study has been on the beam loading of the electron beam. In order to eliminate other factors that may affect this (add examples?), we have tried several approaches to create a stable drive beam structure based on previous self-modulation studies.

Our first approach was to use a pre-modulated, short proton beam with similar structure to the one produced by the self-modulation of the SPS beam in AWAKE. These studies were done using the full PIC code Osiris [17] using 2D cylindrical-symmetric simulations [16, 18].

In order to study the witness beam emittance evolution we turned to the recently released open source ver-

sion of QuickPIC developed by UCLA. QuickPIC is a fully relativistic 3D quasi-static PIC code [19, 20]. Since QuickPIC is a quasi-static code, it does not suffer from the numerical Cherenkov effect that full PIC codes do [21, 22], making it a well suited code to study emittance preservation.

A. Drive Beam Parameters

In these simulations we use a single proton drive beam that sets up a wakefield comparable to that which we expect to see from the self-modulated SPS beam in the second plasma cell of AWAKE Run 2 (Figure 1). When the initial SPS beam containing 3×10^{11} protons [13] enters the second plasma cell, the peak E_z field is expected to be 500–600 MV/m. As the baseline AWAKE drive beam current is insufficient to reach the non-linear regime and produce a plasma bubble, the plasma electrons are only depleted to around 65% of nominal plasma density at the point where we inject the electron beam [23]. These conditions are replicated in our simulations using a single proton beam of 1.46×10^{10} protons, or 2.34 nC and 7 kA.

The peak density of the simulation drive beam is $0.83 \cdot n_0$, producing a quasi-linear wakefield. The single bunch setup uses the baseline proton energy $W_{pb} = 400$ GeV and transverse size $\sigma_x = 200 \mu\text{m}$. We also set the length of the drive beam to $\sigma_z = 40 \mu\text{m}$. In order to create a stable environment to study the evolution of the witness beam we in addition prevented the proton beam from evolving radially by increasing the particle mass by a factor of $1e6$. We are not considering the evolution of the proton beam itself in this study.

B. Witness Beam Parameters

The witness beam in our simulations differs from AWAKE baseline parameters on several key points. Initial beam energy is set such that $\gamma_{eb} = \gamma_{pb} = 426.3$. This was done to eliminate the problem of initial de-phasing of the witness beam. Beam loading of a short witness beam is sensitive to its position relative to the field [24]. The relative drift causing the de-phasing is proportional to γ^{-2} . By simply matching the initial γ values we eliminate this effect entirely, but a lower initial value is likely to be sufficient [16].

In these 3D simulations we have used a matched beam for an initial emittance of $2 \mu\text{m}$, corresponding to a σ_x of $5.25 \mu\text{m}$. The beam matching relation is given by

$$\beta = \frac{\sigma_r^2}{\epsilon_g} = \frac{\lambda_{pe}}{2\pi} \sqrt{2\gamma}, \quad (1)$$

where λ_{pe} is the plasma wavelength and γ is the beam relativistic factor. This relation requires a very narrow beam compared to the drive beam $\sigma_x = 200 \mu\text{m}$. The charge density of this compact witness beam reaches that

of the plasma density at only a few pC, but reaches optimal beam loading at around 1 – 200 pC. The implication here being that the witness beam produces its own non-linear wakefield already at the head of the beam. The majority of the electrons within it will therefore see a linear focusing force preventing the bulk of the beam from undergoing emittance growth.

The relatively small size of the witness beam compared to the proton beam put some restrictions on the transverse resolution of the witness beam. We used a transverse grid cell size of $1.17\ \mu\text{m}$, and $2.34\ \mu\text{m}$ for the longitudinal grid cells. The witness beam was simulated with 16.8 M non-weighted particles. For the largest parameter scans, shown in figure 7, we used a transverse grid cell size of $2.34\ \mu\text{m}$.

In the following section we study a witness beam with a total charge of 100 pC, a $\sigma_z = 60\ \mu\text{m}$, and with a $\sigma_x = 5.23\ \mu\text{m}$ matching an initial normalised emittance $\epsilon_0 = 2\ \mu\text{m}$. We refer to this parameter set as our base case.

III. BEAM LOADING

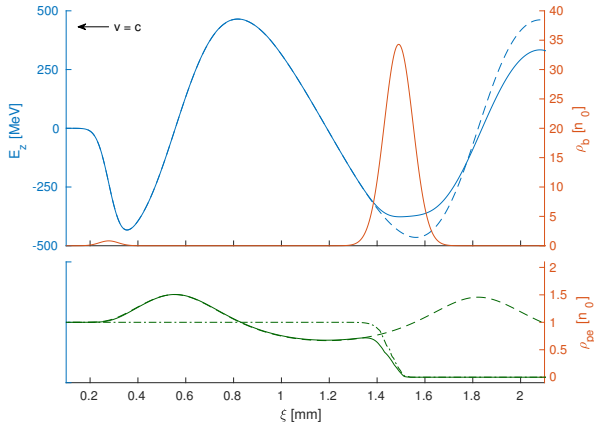


FIG. 2. The top plot compares the unloaded longitudinal e-field (no witness beam, blue. dashed line) and the loaded e-field (blue line) along the beam axis. The magnitude of the beam density along the axis is shown (red line) for reference. The bottom plot compares the plasma density along the beam axis for a drive beam with no witness beam (dashed green line), witness beam with no drive beam (dash-dotted green line), and both witness and drive beam present (continuous green line). $\xi = z - tc$ is the position in the simulation box, and both beams travel towards the left. The beam and plasma densities are in units of initial plasma density $n_0 = 7 \times 10^{-14}\ \text{cm}^{-3}$.

The single drive beam setup is designed to behave similarly to the self-modulated case. However, since the drive beam is prevented from significant transverse evolution, we are presented with an idealised case where the electron witness beam sees consistent wakefields throughout

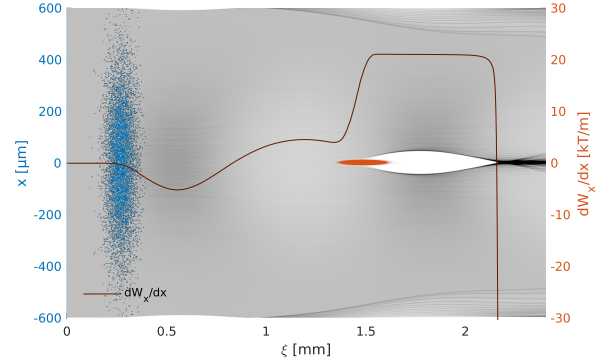


FIG. 3. The plasma density in grey with the proton beam (blue) and the electron beam (red) superimposed. The superimposed line plot indicates the transverse wakefield gradient dW_x/dx where $W_x = E_x - v_b B_y$, evaluated along the beam axis.

the plasma stage. The E_z -field generated by the proton drive beam is seen as the blue line in figure 2, shown with and without the electron beam present. With a proton beam density $n_{pb} \simeq n_0$, we are in the quasi-linear regime but near non-linear [25]. The dashed green line in the lower part of figure 2 shows that the on-axis plasma density has a depletion of 67%, close to what we see in full scale reference simulations for AWAKE Run 2 [23].

The witness beam generates its own wakefield which partially cancels out the E_z field generated by the drive beam. With an ideally shaped electron beam charge profile it is possible to optimally load the field in such a way that the accelerating E_z is constant along the bunch [6, 24].

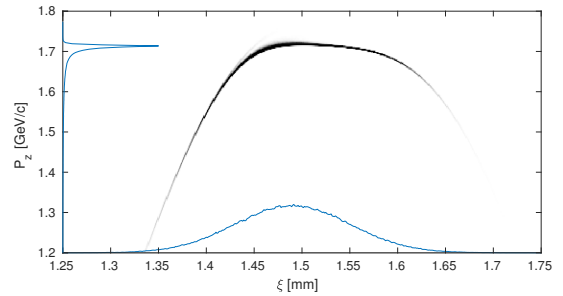


FIG. 4. Phase space charge distribution of a 100 pC, $60\ \mu\text{m}$ long witness beam after 4 m of plasma. Mean momentum is $1.67\ \text{GeV}/c$ with an RMS spread of $87\ \text{MeV}/c$ (5.2%) for the full beam.

While the ideal shape is trapezoidal, for Gaussian beams a reasonable flat field, and consequently low energy spread, can be achieved by controlling the charge density to achieve a similar effect. This, however, puts the front of the witness beam outside of the ideal region while the middle bulk of the beam has a trapezoidal-like

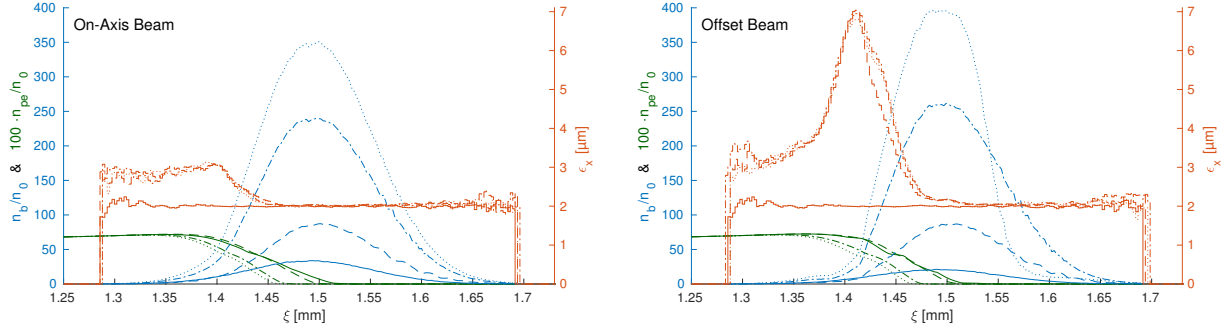


FIG. 5. The red lines show a moving window calculation of transverse normalised emittance for an on-axis beam with respect to the drive beam axis (left), and an offset beam (right) with an offset of one $\sigma_x = 5.24 \mu\text{m}$ in the x-plane. The moving window for emittance calculation is longitudinal slices of $l = 4 \times \Delta\xi = 9.38 \mu\text{m}$ with a $\Delta\xi$ resolution. Only slices with more than 100 macro particles have been included. The blue lines show the on-axis electron beam density profile. For reference, the plasma density profile is included in green, but scaled up by a factor of 100 to be visible. The solid lines are taken at the plasma entry point, the dashed lines after 4 m of plasma, the dash-dotted after 40 m, and the dotted after 100 m. In order to sustain a stable accelerating field for the witness beam, these simulations were run with an LHC energy drive beam of 7 TeV to avoid de-phasing which otherwise causes the structure to break down after about 50 m of plasma.

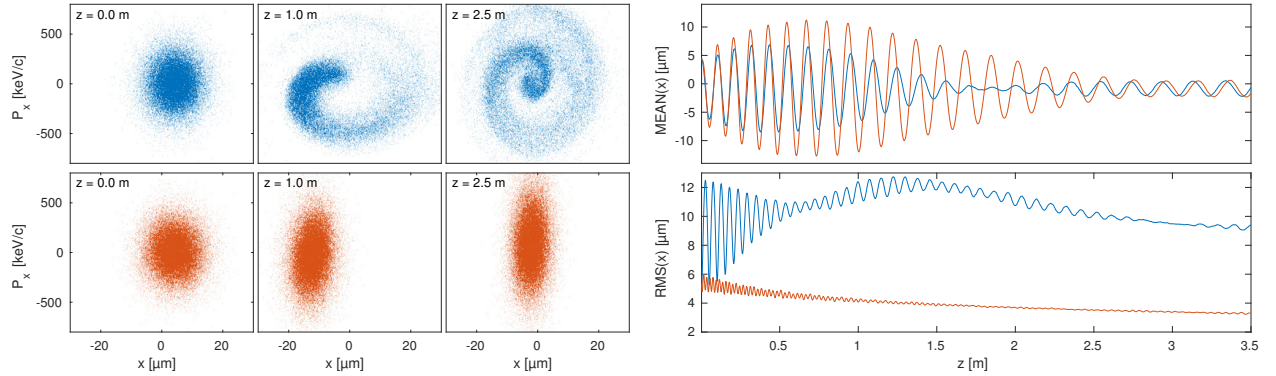


FIG. 6. The left plots show the transverse phase space of the electron beam at different plasma positions. The Right side shows the macro particle mean position (top) and RMS spread (bottom). The blue particles and lines represent particles with position $1.40 \mu\text{m} < \xi < 1.42 \mu\text{m}$. The red particles and lines represent particles with position $1.55 \mu\text{m} < \xi < 1.57 \mu\text{m}$.

shape. In our case, with a matched beam to the plasma density defined by equation 1, we are limited on how much total charge we can accelerate without reaching charge densities that will overload the field.

As illustrated in figure 4 our base case shows a difference in energy transfer to the tail of the beam compared to the centre where the E_z -field is nearly flat. In addition, the front of the beam has a large tail in momentum space as this regions sees a smaller accelerating field. The positioning of the witness beam is chosen to put the bulk of the charge as close to the peak accelerating field as possible.

The charge density required to optimally load the E_z field is $n_{eb} \approx 35 \times n_0$. This means that the witness beam's own wakefield is in the fully non-linear regime, where the space charge force is sufficient to blow-out all plasma electrons resulting in an ion column. This ion column, as

is well known [26], provides a linear focusing force on the part the electron beam within the column, and therefore prevents emittance growth for this region of the beam. This effect is shown for our base case in figure 3. The focusing field has a gradient of 20 kT/m near the beam axis.

For the majority of the cases we studied that maintained a stable accelerating structure, about 70 – 80% of the beam retained its initial emittance. Figure 5 shows emittance growth for the base case as a function of propagation length. No significant emittance growth was observed for propagation lengths up to 100 m. The drive beam energy was here increased to 7 TeV (LHC energy) to prevent de-phasing, as de-phasing starts to become a significant effect for the SPS beam after about 50 m.

The on-axis density of the electron beam increases as its gamma factor increases and its transverse size de-

creases. The beam radius follows the evolution given by equation 1 with $\lambda_{pe} = \lambda_0$ for the section of the beam where normalised emittance is preserved – as shown in figure 6. This has the potential to cause overloading of the field. However, for our base case this effect was not significant.

Since the accelerated electron beam creates its own focusing bubble, the emittance of the part of the beam inside the bubble is not affected by small beam offsets with respect to the proton beam axis. This is an added benefit of this new accelerating regime, and may ease the transverse injection tolerances. The head of the beam does not benefit from this effect, but since the proton beam creates a quasi linear wake, the head of the beam still stabilises after some time. This is illustrated on figure 5 for an electron beam offset of $1\sigma_x$. In this case there is a larger initial emittance growth (see left hand plots of figure 6), but the emittance growth stop after the first few metres (figure 5). This effect is likely to be greater for larger offsets as the beam oscillates around the axis of the drive beam wakefield, as can be seen from the right hand plots of figure 6.

IV. PARAMETER OPTIMISATION

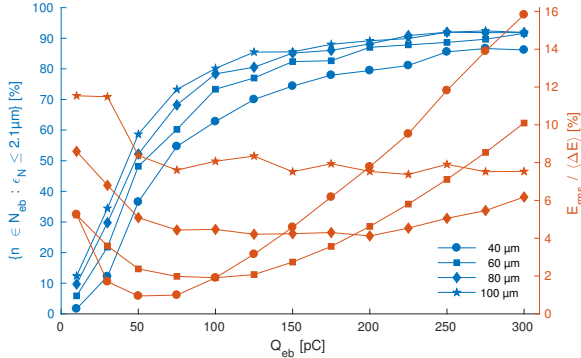


FIG. 7. Ratio of total beam charge with an emittance growth $\Delta\epsilon \leq 5\%$ as a function of initial beam charge (blue), and relative energy spread of the accepted charge (red), after 4 m of plasma and with an initial emittance $\epsilon_{N,0} = 2 \mu\text{m}$. These are shown for four different σ_z from $40 \mu\text{m}$ to $100 \mu\text{m}$. The detailed studies presented in beam loading section correspond to the square marked lines at 100 pC .

The beam loading and blow out properties of the electron beam depends on a large number of parameters: the longitudinal profile, the transverse profile as well as the relative phasing of the proton and the electron beams.

We here study parameter optimization relevant for AWAKE Run 2, in order to understand the ideal injection parameters. For AWAKE Run 2 we desire to maximize the energy gain, minimize the energy spread, maximize the charge to be accelerated and minimize the

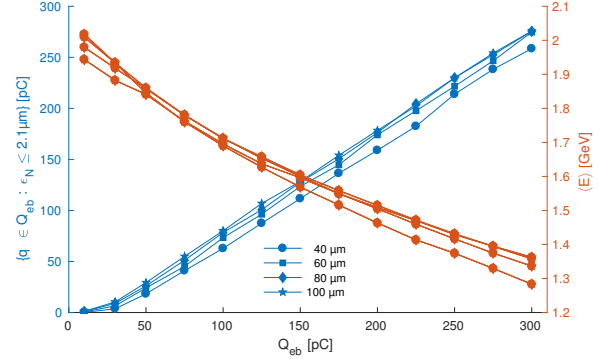


FIG. 8. Total beam charge with an emittance growth $\Delta\epsilon \leq 5\%$ as a function of initial beam charge (blue), and final momentum (red), after 4 m of plasma and with an initial emittance $\epsilon_{N,0} = 2 \mu\text{m}$.

emittance growth. In addition, the bunch length should be such that it is possible to generate and transport by a compact electron injector [15]. These are contradictory constraints. We investigate the interdependence of these parameters by simulation. We vary the electron bunch length, charge and initial emittance. We quantify the resulting emittance growth, energy spread and energy gain. The desired injection parameters will depend on the application.

Figures 7 and 8 show the dependence on bunch length and bunch charge for an initial beam emittance of $2 \mu\text{m}$ after propagating through 4 m of plasma. We ran the scan with beam charges from 10 pC to 300 pC and with length σ_z from $40 \mu\text{m}$ to $100 \mu\text{m}$. We see from figure 7 that both the $40 \mu\text{m}$ and the $60 \mu\text{m}$ beam has a well defined minimum energy spread with a beam charge $\geq 50 \text{ pC}$ and $\approx 100 \text{ pC}$ respectively. Lower beam charges tend to underload the E_z -field, while higher beam charges tend to overload it. It is also clear that long beams with respect to the accelerating flank of the E_z -field, $\approx \lambda_{pe}/4$, will not optimally load the field along its length, thus producing a larger spread in energy.

Figure 9 shows how the growth in emittance and energy spread varies with initial electron beam emittance. The smaller the initial emittance is, the better the emittance is preserved. There are two effects that lead to growth for high emittance beams; the transverse beam size may increase beyond the size of the bubble, or the beam density may be reduced so much that the plasma electrons are no longer fully evacuated from the ion column. Emittance values higher than a few micrometres lead to a significant increase in both emittance and energy spread. In these simulations the focusing of the beam to the plasma remains matched for each emittance value.

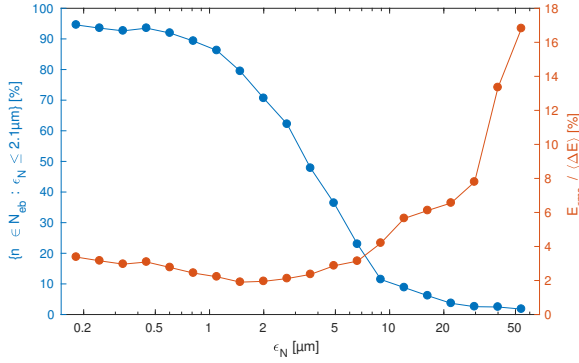


FIG. 9. Ratio of total beam charge with an emittance growth $\Delta\epsilon \leq 5\%$ as a function of initial emittance (blue), and relative energy spread of the accepted charge (red), after 4 m of plasma.

V. CONCLUSION

We have studied a new plasma wakefield acceleration regime; acceleration of a strongly loaded electron beam in a quasi-linear proton driven wake. When optimally loaded, the electron beam creates its own ion bubble, yielding emittance preservation for a large parts of the electron beam.

These result indicates that emittance preservation for an on-axis injected electron beam, properly optimized,

is feasible. Parameter studies indicate that up to a few 100 pC might be accelerated, for bunches of length 40 – 60 μm . Such an electron bunch may be generated by a standard S-band RF gun.

As this study assumes a wake driven by a single, short proton beam, the studies for interesting cases for AWAKE should be repeated by a full simulation of a self-modulated proton beam.

VI. ACKNOWLEDGEMENTS

The simulations for this study have been run using the open source version of QuickPIC released in early 2017 and owned by UCLA.

These numerical simulations have been made possible through access to the Abel computing cluster in Oslo, Norway. Abel is maintained by UNINETT Sigma2 AS and financed by the Research Council of Norway, the University of Bergen, the University of Oslo, the University of Troms and the Norwegian University of Science and Technology. Project code: nn9303k. Some of the simulations were also run on the student-maintained computing cluster “Smaug” at the University of Oslo, Department of Physics.

The authors would also like to acknowledge the OSIRIS Consortium for providing access to the OSIRIS framework. OSIRIS was used extensively for simulations leading up to the work presented in this paper.

-
- [1] P. Chen, J. M. Dawson, R. W. Huff, and T. Katsouleas, *Physical Review Letters* **54**, 693 (1985).
 - [2] J. B. Rosenzweig, D. B. Cline, B. Cole, H. Figueroa, W. Gai, R. Konecny, J. Norem, P. Schoessow, and J. Simpson, *Physical Review Letters* **61**, 98 (1988).
 - [3] I. Blumenfeld, C. E. Clayton, F.-J. Decker, M. J. Hogan, C. Huang, R. Ischebeck, R. Iverson, C. Joshi, T. Katsouleas, N. Kirby, W. Lu, K. A. Marsh, W. B. Mori, P. Muggli, E. Oz, R. H. Siemann, D. Walz, and M. Zhou, *Nature* **445**, 741 (2007).
 - [4] E. Kallos, T. Katsouleas, W. D. Kimura, K. Kusche, P. Muggli, I. Pavlishin, I. Pogorelsky, D. Stolyarov, and V. Yakimenko, *Physical Review Letters* **100**, 074802 (2008).
 - [5] AWAKE Collaboration, R. Assmann, R. Bingham, T. Bohl, C. Bracco, B. Buttenschön, A. Butterworth, A. Caldwell, S. Chattopadhyay, S. Cipiccia, E. Feldbaumer, R. A. Fonseca, B. Goddard, M. Gross, O. Grulke, E. Gschwendtner, J. Holloway, C. Huang, D. Jaroszynski, S. Jolly, P. Kempkes, N. Lopes, K. Lotov, J. Machacek, S. R. Mandry, J. W. McKenzie, M. Meddahi, B. L. Milityn, N. Moschuering, P. Muggli, Z. Najmudin, T. C. Q. Noakes, P. A. Norreys, E. Oz, A. Pardons, A. Petrenko, A. Pukhov, K. Rieger, O. Reimann, H. Ruhl, E. Shaposhnikova, L. O. Silva, A. Sosedkin, R. Tarkeshian, R. M. G. N. Trines, T. Tückmantel, J. Vieira, H. Vincke, M. Wing, and G. Xia, *Plasma Physics and Controlled Fusion* **56**, 084013 (2014).
 - [6] T. Katsouleas, S. Wilks, P. Chen, J. M. Dawson, and J. J. Su, *Particle Accelerators* **22**, 81 (1987).
 - [7] W. Lu, C. Huang, M. Zhou, W. B. Mori, and T. Katsouleas, *Physical Review Letters* **96**, 165002 (2006).
 - [8] W. Lu, C. Huang, M. Zhou, M. Tzoufras, F. S. Tsung, W. B. Mori, and T. Katsouleas, *Physics of Plasmas* (1994-present) **13**, 056709 (2006).
 - [9] P. Muggli, B. Allen, Y. Fang, V. Yakimenko, M. Fedurin, K. Kusche, M. Babzien, C. Swinson, and R. Malone, in *Proceedings of PAC2011* (New York, NY, USA, 2011) pp. 712–714.
 - [10] A. Caldwell, K. Lotov, A. Pukhov, and F. Simon, *Nature Physics* **5**, 363 (2009).
 - [11] S. Steinke, J. van Tilborg, C. Benedetti, C. G. R. Geddes, C. B. Schroeder, J. Daniels, K. K. Swanson, A. J. Gonsalves, K. Nakamura, N. H. Matlis, B. H. Shaw, E. Esarey, and W. P. Leemans, *Nature* **530**, 190 (2016).
 - [12] C. A. Lindström, E. Adli, J. M. Allen, J. P. Delahaye, M. J. Hogan, C. Joshi, P. Muggli, T. O. Raubenheimer, and V. Yakimenko, *Nuclear Instruments and Methods in Physics Research Section A* **829**, 224 (2016).
 - [13] E. Gschwendtner, E. Adli, L. Amorim, R. Apsimon, R. Assmann, A. M. Bachmann, F. Batsch, J. Bauche, V. K. Berglyd Olsen, M. Bernardini, R. Bingham,

- B. Biskup, T. Bohl, C. Bracco, P. N. Burrows, G. Burt, B. Buttenschön, A. Butterworth, A. Caldwell, M. Cascella, E. Chevallay, S. Cipiccia, H. Damerau, L. Deacon, P. Dirksen, S. Doeber, U. Dorda, J. Farmer, V. Fedosseev, E. Feldbaumer, R. Fiorito, R. Fonseca, F. Friebel, A. A. Gorn, O. Grulke, J. Hansen, C. Hessler, W. Hofle, J. Holloway, M. Hüther, D. Jaroszynski, L. Jensen, S. Jolly, A. Joulaei, M. Kasim, F. Keeble, Y. Li, S. Liu, N. Lopes, K. V. Lotov, S. Mandry, R. Martorelli, M. Martyanov, S. Mazzoni, O. Mete, V. A. Minakov, J. Mitchell, J. Moody, P. Muggli, Z. Najmudin, P. Norreys, E. Öz, A. Pardons, K. Pepitone, A. Petrenko, G. Plyushchev, A. Pukhov, K. Rieger, H. Ruhl, F. Salveter, N. Savard, J. Schmidt, A. Seryi, E. Shaposhnikova, Z. M. Sheng, P. Sherwood, L. Silva, L. Soby, A. P. Sosedkin, R. I. Spitsyn, R. Trines, P. V. Tuev, M. Turner, V. Verzilov, J. Vieira, H. Vincke, Y. Wei, C. P. Welsch, M. Wing, G. Xia, and H. Zhang, *Nuclear Instruments and Methods in Physics Research Section A* **829**, 76 (2016).
- [14] N. Kumar, A. Pukhov, and K. Lotov, *Physical Review Letters* **104**, 255003 (2010).
- [15] E. Adli and AWAKE Collaboration, in *Proceedings of IPAC 2016*, International Particle Accelerator Conference (JACoW, Busan, Korea, 2016) pp. 2557–2560.
- [16] V. K. Berglyd Olsen, E. Adli, P. Muggli, L. D. Amorim, and J. Vieira, in *Proceedings of IPAC 2015* (Richmond, VA, USA, 2015) pp. 2551–2554.
- [17] R. A. Fonseca, L. O. Silva, F. S. Tsung, V. K. Decyk, W. Lu, C. Ren, W. B. Mori, S. Deng, S. Lee, T. Katsouleas, and J. C. Adam, in *Computational Science — ICCS 2002*, Lecture Notes in Computer Science No. 2331, edited by P. M. A. Sloot, A. G. Hoekstra, C. J. K. Tan, and J. J. Dongarra (Springer Berlin Heidelberg, 2002) pp. 342–351.
- [18] V. K. Berglyd Olsen, E. Adli, P. Muggli, and J. Vieira, in *Proceedings of NAPAC 2016* (Chicago, IL, USA, 2016).
- [19] C. Huang, V. K. Decyk, C. Ren, M. Zhou, W. Lu, W. B. Mori, J. H. Cooley, T. M. Antonsen, and T. Katsouleas, *Journal of Computational Physics* **217**, 658 (2006).
- [20] W. An, V. K. Decyk, W. B. Mori, and T. M. Antonsen, *Journal of Computational Physics* **250**, 165 (2013).
- [21] B. B. Godfrey, *Journal of Computational Physics* **15**, 504 (1974).
- [22] R. Lehe, A. Lifschitz, C. Thaur, V. Malka, and X. Davoine, *Physical Review Special Topics - Accelerators and Beams* **16**, 021301 (2013).
- [23] AWAKE Collaboration and A. Caldwell, *AWAKE Status Report, 2016*, Tech. Rep. CERN-SPSC-2016-033 (CERN, Geneva, 2016).
- [24] M. Tzoufras, W. Lu, F. S. Tsung, C. Huang, W. B. Mori, T. Katsouleas, J. Vieira, R. A. Fonseca, and L. O. Silva, *Physics of Plasmas* **16**, 056705 (2009).
- [25] J. B. Rosenzweig, G. Andonian, M. Ferrario, P. Muggli, O. Williams, V. Yakimenko, and K. Xuan, *AIP Conference Proceedings* **1299**, 500 (2010).
- [26] J. B. Rosenzweig, B. Breizman, T. Katsouleas, and J. J. Su, *Physical Review A* **44**, R6189 (1991).

Appendices

Appendix A

Particle in Cell (PIC)

Some stuff about PIC codes

A.1 Numerical Cherenkov

Appendix B

Data Analysis

It has been very useful to develop a tool for effective analysis of the large amount of data produced by the Osiris and QuickPIC simulations used in this study. Most of the initial studies have been done using Osiris, and while the emittance studies have been mostly done using QuickPIC.

For the experiment itself a portion of the PhD project has been spent developing data acquisition tools and integrating these with the existing CERN data acquisition infrastructure.

As of the time of writing, the OsirisAnalysis framework is publicly available on GitHub¹.

B.1 Osiris Analysis Framework

The OsirisAnalysis framework is a modular and object oriented data analysis framework written in MATLAB. It was designed as a three layer tool to wrap a single data set of OSIRIS simulation data.

- **Layer 1:** Consists of the core datawrapper, `OsirisData`, which provides an interface through which raw data files as well as the simulation input file is parsed. It provides a uniform method for extracting data, and gives access to all the simulation parameters and conversion factors for converting Osiris' normalised units into SI units.
- **Layer 2:** The second layer consists of a set of classes that takes an `OsirisData` object as input, and returns standardised structs of data that can be scaled and converted to preferred units. They perform often needed tools and methods to parse data and extract more detailed information from the larger raw datasets.
- **Layer 3:** The third layer consists of a number of useful standardised plots and a GUI tool to quickly do a preliminary analysis of simulation data.

The philosophy behind this layering of the analysis tool is to allow the user the freedom to choose how many of these they will use. Only using the first layer will give the user access to all the simulation parameters as well as a method to extract data in a standardised manner and return a simple matrix of its content. Adding the second layer gives additional access to automatic unit conversion and other tools if needed. The third layer is entirely optional and simply provides a quick way to browse through the data.

B.1.1 OsirisAnalysis Core Objects

The innermost layer consists of two classes `OsirisData` and `OsirisConfig`.

The `OsirisData` class wraps the simulation data folder and is the core interface through which data is extracted. The class also provides some simple methods for extracting information about the dataset like physical dimensions of the beam and the distribution of the plasma.

The `OsirisConfig` class is a wrapper for the input file itself, and contains a parser for this file which extracts all the relevant information for both analysis and provides lists of available diagnostics for the graphical user interface (GUI). All conversion factors to SI units are calculated on the fly when the input file is loaded. The `OsirisConfig` class is not intended to be called by the user, but is found as a child object of the `OsirisData` data object.

B.1.2 OsirisAnalysis Data Types

The secondary layer of the `OsirisAnalysis` framework is a set of subclasses under a parent class named `OsirisType`. The subclasses will give access to specific types of data more or less directly related to the diagnostics types produced by the OSIRIS simulation code.

The classes provided are:

- **Density and Field:** These are classes that produce grid diagnostics data for the particle density data dumps or the field diagnostics data. They support all the different density diagnostics outputs of Osiris, and will in addition calculate the wakefields from the magnetic and electric fields given by $W = F/q = E - v \times B$.
- **Momentum:** The Momentum class consists of a set of methods that will calculate the evolution of the beams energy and momentum over several time dumps.
- **Phase:** The Phase class provides several tools for phase space diagnostics, including calculations of Twiss parameters.
- **UDist:** This class is similar to the Dnesity and Field classes, and provides methods to process velocity and thermal distribution data.
- **Species:** The Species class provides a few additional specialised tools for calculating energy deposition and gain into and from the plasma by the beams, and is also the class where particle tracking data is parsed.

In addition to these data parsing classes, there is also a `Variables` class that will translate Osiris diagnostics variables into readable forms and into strings usable for plot labels. There is also a `MathFunc` class that provides a math parser that emulates the one used by OSIRIS to parse mathematical functions from the input files. This class is mainly used to extract geometric information about beam density based on the function provided in the input file without the need to first run the code to provide raw particle data.

B.1.3 OsirisAnalysis Graphical Interface and Plots

The final layer of the `OsirisAnalysis` framework is a set of very flexible plotting tools. Most of them have a long list of optional input argument. Most of these optional arguments are available through a graphical interface also written in MATLAB named `AnalysisGUI`.

Bibliography

- [1] V. K. Berglyd Olsen. [OsirisAnalysis: Matlab Analysis Code for Osiris Simulations](https://github.com/Jadzia626/OsirisAnalysis). GitHub Repository, 2013. <https://github.com/Jadzia626/OsirisAnalysis>.
- [2] V. K. Berglyd Olsen, E. Adli, P. Muggli, L. D. Amorim, and J. Vieira. [Loading of a Plasma-Wakefield Accelerator Section Driven by a Self-Modulated Proton Bunch](#). In *Proceedings of IPAC 2015*, pages 2551–2554, Richmond, VA, USA, May 2015. ISBN 978-3-95450-168-7.
- [3] V. K. Berglyd Olsen, E. Adli, P. Muggli, and J. Vieira. Loading of Wakefields in a Plasma Accelerator Section Driven by a Self-Modulated Proton Beam. In *Proceedings of NAPAC 2016*, Chicago, IL, USA, Oct. 2016.
- [4] V. K. Berglyd Olsen, J. J. Batkiewicz, S. Deghaye, S. J. Gessner, E. Gschwendtner, and P. Muggli. [Data Acquisition and Controls Integration of the AWAKE Experiment at CERN](#). In *Proceedings of IPAC2017*, Copenhagen, Denmark, May 2017.
- [5] I. Blumenfeld, C. E. Clayton, F.-J. Decker, M. J. Hogan, C. Huang, R. Ischebeck, R. Iversen, C. Joshi, T. Katsouleas, N. Kirby, W. Lu, K. A. Marsh, W. B. Mori, P. Muggli, E. Oz, R. H. Siemann, D. Walz, and M. Zhou. [Energy doubling of 42 GeV electrons in a metre-scale plasma wakefield accelerator](#). *Nature*, 445(7129):741–744, Feb. 2007. ISSN 0028-0836. doi:[10.1038/nature05538](https://doi.org/10.1038/nature05538).
- [6] H. H. Braun, S. Döbert, I. Wilson, and W. Wuensch. [Frequency and Temperature Dependence of Electrical Breakdown at 21, 30, and 39 GHz](#). *Physical Review Letters*, 90(22): 224801, June 2003. doi:[10.1103/PhysRevLett.90.224801](https://doi.org/10.1103/PhysRevLett.90.224801).
- [7] P. Chen, J. M. Dawson, R. W. Huff, and T. Katsouleas. [Acceleration of Electrons by the Interaction of a Bunched Electron Beam with a Plasma](#). *Physical Review Letters*, 54(7): 693–696, Feb. 1985. doi:[10.1103/PhysRevLett.54.693](https://doi.org/10.1103/PhysRevLett.54.693).
- [8] E. Kallos, T. Katsouleas, W. D. Kimura, K. Kusche, P. Muggli, I. Pavlishin, I. Pogorelsky, D. Stolyarov, and V. Yakimenko. [High-Gradient Plasma-Wakefield Acceleration with Two Subpicosecond Electron Bunches](#). *Physical Review Letters*, 100(7):074802, Feb. 2008. doi:[10.1103/PhysRevLett.100.074802](https://doi.org/10.1103/PhysRevLett.100.074802).
- [9] D. P. Pritzkau and R. H. Siemann. [Experimental Study of RF Pulsed Heating on Oxygen Free Electronic Copper](#). *Physical Review Special Topics - Accelerators and Beams*, 5(11): 112002, Nov. 2002. doi:[10.1103/PhysRevSTAB.5.112002](https://doi.org/10.1103/PhysRevSTAB.5.112002).

- [10] J. B. Rosenzweig, D. B. Cline, B. Cole, H. Figueroa, W. Gai, R. Konecny, J. Norem, P. Schoessow, and J. Simpson. [Experimental Observation of Plasma Wake-Field Acceleration](#). *Physical Review Letters*, 61(1):98–101, July 1988. doi:[10.1103/PhysRevLett.61.98](#).
- [11] S. Van der Meer. [Improving the power efficiency of the plasma wakefield accelerator](#). Technical Report CERN/PS/85-65 (AA), CLIC Note No. 3, CERN, Geneva, Nov. 1985.